



Velocity fields and depositional processes in laboratory ash flows, with implications for the dynamics of dense pyroclastic flows

L Girolami, Olivier Roche, T. Druitt, T Corpetti

► To cite this version:

L Girolami, Olivier Roche, T. Druitt, T Corpetti. Velocity fields and depositional processes in laboratory ash flows, with implications for the dynamics of dense pyroclastic flows. *Bulletin of Volcanology*, 2010. hal-02169477

HAL Id: hal-02169477

<https://hal.science/hal-02169477>

Submitted on 1 Jul 2019

HAL is a multi-disciplinary open access archive for the deposit and dissemination of scientific research documents, whether they are published or not. The documents may come from teaching and research institutions in France or abroad, or from public or private research centers.

L'archive ouverte pluridisciplinaire **HAL**, est destinée au dépôt et à la diffusion de documents scientifiques de niveau recherche, publiés ou non, émanant des établissements d'enseignement et de recherche français ou étrangers, des laboratoires publics ou privés.

Velocity fields and depositional processes in laboratory ash flows, with implications for the dynamics of dense pyroclastic flows

L.Girolami^{1*}, O. Roche¹, T.H. Druitt¹ and T. Corpetti²

¹ Laboratoire Magmas et Volcans, Université Blaise Pascal-CNRS-IRD, 5 rue Kessler, 63038 Clermont-Ferrand, France.

² Equipe C.O.S.T.E.L, Université Rennes II, CNRS-IRISA-INRIA, Place du Recteur Henri Le Moal, 35043 Rennes, France.

** Corresponding author*

Abstract

We conducted laboratory experiments on dam-break flows of sub-250- μm volcanic ash, generated by the release of gas-fluidized and variably non-expanded to expanded (up to 35%) beds, in order to gain insights into the kinematics of pyroclastic flows. The flows were typically several cm thick, had frontal speeds of up to $\sim 2 \text{ m s}^{-1}$, and were non-turbulent on scales larger than the constituent particles. High-speed videos taken through the transparent sidewall of the 3-m-long channel were analyzed with a particle-tracking algorithm, providing a spatial and temporal description of transport and sedimentation. The flows deposited progressively as they traveled down the flume, being consumed by sedimentation until they ran out of volume. Deposition commenced 5-20 cm rearward of the flow front and (for a given expansion) proceeded at a rate independent of distance from the lock gate. Deposit aggradation velocities were equal to those inferred beneath quasi-static bed collapse tests of the same ash at the same initial expansions, implying that shear rates of up to $\sim 300 \text{ s}^{-1}$ have no measurable effect on aggradation rate. The initially non-expanded (and just fluidized) flow deposited progressively at a rate indicative of an expansion of a few percent, perhaps due to Reynolds dilation during initial slumping. The fronts of the flows slid across the flume floor on very thin basal shear layers, but once deposition commenced, a no-slip condition was established at the depositional interface. Velocity increased with height above the depositional interface, reached a maximum, then declined slightly towards the flow surface, perhaps due to air drag. At a given location, the velocity profiles were translated upwards as the deposit aggraded. The results show that even cm-thin, non-turbulent and poorly expanded flows of ash deposit progressively, as inferred for many pyroclastic flows. The change from (frontal) slip to (rearward) no-slip conditions at the bases of the laboratory flows are qualitatively consistent with some textural features of pyroclastic flow deposits.

Keywords: Pyroclastic flow, fluidized granular flow, laboratory experiment, velocity profile, progressive aggradation.

Introduction

Pyroclastic flows are dense granular avalanches of hot particles and gas generated by gravitational collapse from lava domes or fallback of eruption columns. They travel at high speeds and constitute one of the most important hazards around active volcanoes (e.g., Wilson 1986; Druitt 1998; Freundt and Bursik 2001). Their ability to travel large distances on slopes as gentle as a few degrees has been attributed to non-equilibrium pore pressures and associated fluidization effects generated either by gases released internally or by entrainment of air (Sparks 1976; Wilson 1980; Druitt et al. 2007). Development of quantitative models of pyroclastic flows is a priority of modern volcanology, and this requires better understanding of their physical properties. While the physics of gravitational dry granular flows (in which it is assumed that particle interactions dominate and that interstitial gas plays a negligible role), has been explored extensively (for reviews, see GDR MiDi 2004 and Forterre and Pouliquen 2008), research on dense gas-particle flows dominated by fluid-particle interactions is much less advanced (Roche et al. 2004, 2008; Girolami et al. 2008).

Up to now the dynamics of pyroclastic flows has been largely based on field observations of active flows (e.g., Hoblitt 1986; Levine and Kieffer 1991), and in particular inferred from textural studies of flow deposits (Sparks 1976; Branney and Kokelaar 2002 and references therein). However in order to use deposits to infer flow dynamics, it is crucial to understand how such deposits form (Branney and Kokelaar 2002). Moreover, pyroclastic flows appear to be capable of a wide spectrum of behaviors, from depositional to strongly erosional, the physics of which are poorly understood.

The kinematics of gas-fluidized particulate flows can be investigated through quantitative analysis of laboratory experiments. Fluidization is the process whereby the drag exerted by an upward flow of gas through a granular bed reduces interparticle stresses, the fluidization state being determined by the vertical superficial gas velocity U_g (gas volumetric flux divided by surface area at the temperature of operation) (Rhodes 1998). Once U_g exceeds a minimum fluidization value U_{mf} , gas drag balances particle weight, friction disappears, and the bed adopts a liquid-like behavior. Some fine-grained powders (group A of Geldart 1973) expand uniformly between U_{mf} and the minimum bubbling threshold, U_{mb} ($>U_{mf}$). If the gas supply to a uniformly expanded bed is cut, the bed re-sediments from the base upwards by hindered settling in what is called a bed collapse (Lettieri et al. 2000; Druitt et al. 2007). Laboratory studies of dense gravitational gas-particle flows include those of both continuously fluidized flows (Eames and Gilbertson 2000; Takahashi and Tsujimoto 2000; Gilbertson et al. 2008), and dam-break (i.e., transient) flows of initially fluidized particles released from a reservoir and that defluidize progressively during propagation (Roche et al. 2004, 2008; Girolami et al. 2008). Roche et al. (2008) showed that dam-break flows of small ($<100\ \mu\text{m}$) group-A glass beads initially fluidized at U_{mb} (with a corresponding bed expansion of 2-4%) propagate on a horizontal substrate in three distinct phases based on observations of the flow front: (1) a short initial acceleration phase as the reservoir empties, (2) a dominant phase in which the front has an approximately constant velocity $U \sim \sqrt{2gh_0}$, where h_0 is the height of the initial material in the reservoir, and (3) a short stopping phase. Flow behavior during phases 1 and 2, which together account for $\sim 80\%$ of the flow runout, strongly resembles that of inertial fluids such as water (probably because of strong gas-particle interactions), and it is consequently inferred that inertia dominates flow motion during the first two phases of emplacement, while a granular-frictional regime may dominate the third phase (Roche et al. 2008).

Similar experiments were carried out by Girolami et al. (2008) with hot volcanic ash. Hot ash differs from glass beads in that it can be expanded considerably (up to $\sim 40\%$) above loose packing when fluidized above U_{mf} , allowing the effect of initial expansion on flow

kinematics to be investigated. Heating the ash to ~ 200 °C was necessary to reduce interparticle cohesion due to atmospheric humidity, allowing the ash to behave as a group-A material (Druitt et al. 2007). The ash-flow experiments showed that the runouts of initially expanded flows scale with the initial expansion, the first emplacement phase being governed by gravitational acceleration, and the second and third phases being dominated by both gravity and hindered sedimentation. Additional experiments with tracer particles revealed that deposition from initially expanded flows takes place incrementally at the flow base. A major finding of this work was that the upper surface of the deposit aggraded at a mean velocity identical to that inferred to take place at the base of a collapsing quasi-static bed of the same ash, expanded by the same initial amount, in the flume reservoir with the lock gate closed. High rates of shear therefore appeared not to affect deposit aggradation rate under collapsing layers of initially expanded ash.

The aim of the present study is to investigate in more detail the internal kinematics and deposition behavior of experimental flows of volcanic ash similar to those described by Girolami et al. (2008). For this, we made high-speed videos of the experiments, which were subsequently treated with sophisticated techniques of motion field estimation. For a range of initial bed expansions, we analyzed the temporal and spatial development of both the deposit and the velocity profile in the overlying flowing ash. We first present the method of image sequences analysis and the results obtained, then discuss possible implications for the depositional mechanisms and erosive capacities of pyroclastic flows.

Experimental procedures

The high-temperature flume

The experiments were carried out in a linear flume consisting of a fluidization reservoir and a horizontal channel built of aluminium and pyrex in order to withstand temperatures of up to 200° C (Figure 1; see Girolami et al. 2008 for a detailed description). The high temperature was provided by external heating tapes regulated by thermostats and covering both the reservoir and an underlying windbox, and all experiments were carried out with the incoming gas and reservoir contents at the same temperature. The ash was fluidized and expanded in the rectangular reservoir (length 30 cm, height 50 cm) and was subsequently released by means of a lock gate into the channel (length 300 cm, height 30 cm). The width of both the reservoir and the channel was 15 cm. The ash rested on a porous plate of mean pore size of 17 μm that separated the windbox from the reservoir. The gas flux entering the windbox was controlled by flowmeters and was recalculated according to the operating temperature and the ideal gas law. The fluidization state of ash in the reservoir was given by the pressure drop across the bed measured by a pressure transducer. By means of a three-way valve, the incoming gas could be either directed into the windbox or vented outward during bed collapse tests as the gas supply was suddenly cut. The reservoir gate had a 20-kg counterweight allowing upward motion at a consistently high speed, and had a heat-resistant seal and a downward-tapering shape to prevent leakage and reduce resistance during opening. Releasing the fluidized ash across the impermeable floor of the flume in the manner of a dam-break formed a fast-moving, short-lived, shear current that defluidized progressively during propagation until motion ceased.

Experimental material and procedure

The volcanic ash involved in the experiments was that used by Girolami et al. (2008). It contained a broad spectrum of particle sizes, from ~ 1 to 250 μm , and was obtained by disaggregating the matrix of a 0.58-Ma non-welded trachytic ignimbrite from Neschers

(Massif Central, France) and removing particles $>250\ \mu\text{m}$. The ash was then fluidized in the flume reservoir in the bubbling regime ($U_g > U_{mb}$), so that the finest particles were elutriated from the bed. The operation was stopped when the elutriation rate became negligible, and this resulted in a slightly fines-depleted material that was subsequently used to generate the flows. We could use the same batch for all experiments since no subsequent elutriation occurred and the grain-size distribution remained constant (see Table 1 in Girolami et al. 2008).

The ash was dried at 200°C during 24 hours before each experiment, then transferred to the lock-gate reservoir where it was fluidized and expanded as required. The operating temperature of all experiments was fixed at 170°C , which was high enough to avoid humidity-related cohesive effects (Druitt et al. 2007). All experiments were limited to the non-bubbling state ($U_{mf} \leq U_g < U_{mb}$), and the bed expansion was defined as

$$E = h_0/h_{mf}, \quad (1)$$

where h_0 and h_{mf} are respectively the expanded and non-expanded (i.e., at U_{mf}) heights of initial bed of ash (Figure 1). Under these conditions, the maximum value of E (at U_{mb}) was 1.45.

No detectable particle-size segregation occurred during expansion or re-sedimentation of the ash, either during quasi-static expansion and collapse in the reservoir, or during horizontal flow, as confirmed by sieving. It is known that even strongly polydisperse suspensions of particles may settle without segregation provided the initial concentration is high enough (Davies and Kaye 1971; Lockett and Al-Habboby 1974; Druitt 1995). This enabled us to assign bulk properties to the ash (e.g., flow velocity, deposit aggradation velocity), and interpret the results quantitatively.

In some experiments, tracer particles of $500\text{-}\mu\text{m}$ silicon carbide (SiC) were added to the ash in proportions up to 10 vol%. This was done to permit visual estimation of particle motions from videos for comparison with those calculated using the optical-flow algorithm. Video footage revealed no disturbance by the tracer particles of the flow or sedimentation dynamics, and this is consistent with previous findings that low amounts of large particles are advected passively in flows of fluidized group-A particles (Roche et al. 2005).

We first studied the hindered settling behavior of the ash under quasi-static (non-shearing) conditions in bed-collapse tests in the reservoir of the apparatus with the gate shut. After expanding the bed to a known amount, we then cut the gas supply and measured the descent rate of the surface (Druitt et al. 2007). The second part of our investigation involved the study of the flows in the channel. Once at temperature, the bed was first mixed to avoid channeling, then mixing was stopped to allow homogeneous bed expansion, and the lock gate was opened by the required amount. The experimental conditions were the same as in experiment series 2 of Girolami et al. (2008): h_{mf} was fixed at 16.5 cm in all experiments, so that h_0 increased proportionally with E and flows were generated at four different values of E : 1.00 (non-expanded), 1.09, 1.17 and 1.35.

Method of velocity-field estimation

Principle of the method

Flow velocity fields and vertical profiles were determined using the particle-tracking technique of Corpetti et al. (2006), which is based on the theory of optical flow. Optical-flow techniques are commonly used in the computer-vision community, and were introduced by Horn and Schunck (1981) for the tracking of rigid objects (particles in the present context) in

image sequences. They allow estimation of a dense motion field (i.e. the velocity at each point of the image) from the intensities (also called luminance) of a pair of consecutive images.

The fundamental principle is to minimize an energy function based on two assumptions: 1) luminance conservation and 2) spatial consistency of the velocity-vector field. The first assumption is that all points of the first image conserve their intensities on the second image. This enables us to use the image pair to generate an estimate of the flow-velocity field. However, in areas of the images where no spatial or temporal variations of luminance are apparent, this leads to an undetermined equation with an infinity of possible solutions. To solve this problem, Horn and Schunck (1981) introduced a spatial-smoothing term that roughly assumes that all neighborhood points have a similar motion (assumption 2). This generates smooth flow fields where spatial gradients of motion are very low.

Our optical-flow method (Corpetti et al. 2006) is a modified version of the original (Horn and Schunck 1981), where instead of generating very smooth flow fields, we estimate velocity vectors where some properties of fluid flows such as divergence and vorticity, are conserved.

Film acquisition and validity of the algorithm

For each experiment, the whole channel was filmed with a standard video camera (25 images per second) to determine the flow front velocity. Parts of the flows were filmed in detail with a high-speed video camera (1000 images per second) placed at a distance that depended on the flow runout, in order to focus the analysis on flow phase 2. The camera was then located at various distances (20-30 cm – 50-60 cm – 80-90 cm – 110-120 cm) from the lock gate, and this was done using a single camera and by repeating each experiment multiple times, as permitted by the high reproducibility of the experiments. Girolami et al. (2008) showed that the flows slipped along the pyrex wall of the channel, so that particle movements observed through the wall were inferred to be representative of the flow interior.

The films were analyzed using the optical-flow algorithm; in each case, a series of velocity fields were determined from motion estimation between two images at a time interval of 1/500 s, which was sufficient for detectable motion. The high-speed video camera was placed 30 cm from the transparent channel wall, so that the algorithm determined particle motion in vertical strips ~10 cm wide. Velocity profiles were then extracted from strips ~1 cm wide perpendicular to the upper surface of the aggrading deposit. Inconsistent velocity fields at flow boundaries due to sidewall-reflection or perspective-related-shadow effects were avoided using a masking technique (Corpetti et al. 2006). Generating the mask consisted of grouping pixels outside the flow and associating them with a color that contrasted markedly with that of the flow, so that the algorithm encountered no ambiguity.

In order to test the validity of the algorithm, we measured the thickness of the basal deposit (i.e., no velocity) as a function of time from videos of ash flows without SiC tracers. For comparison, we also measured the deposit thickness by visual inspection of videos of flows with SiC. Both methods revealed similar results (Figure 2), thus showing that the algorithm was suitable for the aim of our study. This also confirmed that tracer particles had no noticeable influence on deposit aggradation rate.

Results

Bed collapse tests and general flow behavior

The results of the quasi-static bed collapse tests in the reservoir are presented in Figure 3 for initial expansions from 1.06 to 1.43, along with data for flows in the channel that will be discussed later. As observed previously (Druitt et al. 2007; Girolami et al. 2008), the hindered settling velocity (V , in cm s^{-1}) of the ash given by the descent rate of the upper surface increases with E , the best-fit relationship in the present case being :

$$V = 2.44E - 2.15 \quad (2)$$

Note that the value of V for a given E is higher than for the ash of Girolami et al. (2008) (grey region of Figure 3), owing to the presence of the SiC particles.

The general behavior of the flows was described by Girolami et al. (2008). When released, the ash flowed down the channel until defluidization was complete and frontal motion ceased. Propagation took place in the three main phases typical of dam-break granular flows: the first, brief initial acceleration phase (1) lasted 0.1-0.2 s; the second, dominant phase (2) during which the front had an approximately constant velocity lasted 0.6-0.8 s and accounted for about two thirds of the flow duration and 70-80 % of the flow runout; and the third, brief stopping phase (3) lasted 0.1-0.4 s. The non-expanded flow ($E=1.00$) had a phase-2 velocity of $\sim 1.1 \text{ m s}^{-1}$, a runout distance of 0.6 m and a runout duration of 0.8 s, whereas the most expanded flow ($E=1.35$) had a phase-2 velocity of $\sim 2.1 \text{ m s}^{-1}$, a runout distance of 2.2 m and a runout duration of 1.4 s.

Characteristics of velocity fields and profiles

The velocity fields revealed a basal (static) deposit beneath the overriding flow for the whole range of initial bed expansions investigated (Figures 4-7). Sedimentation commenced ~ 0.05 -0.10 s (~ 5 -20 cm) behind the flow front at all distances from the lock gate, and the deposit took the form of a wedge that thickened with time at the expense of the flow until the latter was entirely consumed. The upper surface of the deposit was steeply inclined (up to 20 - 25°) and remained approximately constant with time beneath the initially non-expanded flow ($E=1.00$). In contrast, it was much more gently inclined beneath the initially expanded flows ($E>1.00$), and decreased from 2° to 0.8° as E increased from 1.09 to 1.35. The flow fronts were typically rounded in cross section near the lock gate, but became progressively more triangular in form with increasing distance downstream. Immediately behind the front, the flowing region thickened to a maximum of 3-4 cm, before then decreasing in thickness, both temporally at a given location as the deposit aggraded, and longitudinally down the flume. In the initially expanded flows, the angle of the flow surface was slightly greater than that of the underlying deposit, whereas the reverse was true in the non-expanded flow.

By analogy with pure fluids, flows were “laminar” on scales larger than individual grains. Velocity vectors in the initially expanded flows had significant downward components within 20-25 cm of the lock gate inherited from the initial phase-1 collapse, but beyond this the vectors became sub-horizontal. A downward flow component was maintained to the distal limit in the initially non-expanded flow, owing to the steep surface of the aggrading deposit.

Velocity profiles revealed different flow behaviors before and after the onset of deposition (Figure 8). The fronts of both expanded and non-expanded flows slid along the channel floor on a basal slip zone $< 1 \text{ mm}$ thick with only a weak vertical velocity gradient in the over-riding flow. Once deposition had commenced, however, shear was accommodated more uniformly throughout the flow and velocity increased more progressively towards the deposit surface. In the initially non-expanded flows, velocity increased rapidly upwards over a few mm above the deposit surface, then increased more slowly towards the flow surface and reached a maximum of about 1.6 m s^{-1} . In contrast, in the initially expanded flows, velocity

increased upwards in a quasi-linear manner (though velocity profiles were slightly concave upward), but then decreased again near the flow surface. Maximum velocity increased with E , from 1.6 m s^{-1} ($E=1.09$) to 1.9 m s^{-1} ($E=1.35$), these being similar to the phase-2 frontal velocity in each case. As the deposit aggraded at a given site, the velocity profile was translated upwards while maintaining approximately the same shape. Velocity gradients increased as the flows thinned progressively downstream. Consequently, the highest shear rate estimated 25 cm from the lock gate was $\sim 125\text{--}150 \text{ s}^{-1}$, while that at 85 cm was $\sim 275\text{--}300 \text{ s}^{-1}$.

Aggradation of the basal deposit

Figure 9 shows the evolution of deposit thickness with time for the different flows, $t=0$ marking the passage of the flow front at various distances from the reservoir gate. The formation of the basal deposit started after passage of the front, and the time interval was about 0.05 s for the initially non-expanded ($E=1$) flow, and increased slightly from 0.05 to 0.10 s when as E increased from 1.09 to 1.35. Regarding aggradation of the deposit, the data reveal three main features. First, the mean aggradation velocity was dependent on E . Second, aggradation velocity at each value of E was almost independent of distance down the channel, showing that it was sufficient to measure this parameter at a single location down the flume to obtain representative values. Third, the aggradation velocity (at a given E) was approximately constant with time at each location. Initial aggradation occurred at $\sim 4.9 \text{ cm s}^{-1}$ at $E=1.09$, $\sim 4.1 \text{ cm s}^{-1}$ at $E=1.17$, and $\sim 2.4 \text{ cm s}^{-1}$ at $E=1.35$. In the $E=1.00$ flow, this rate remained constant until sedimentation was complete. In the initially expanded flows, however, there is an indication that aggradation speeded up during the final increments (0.7–0.9 s) of sedimentation, although this behavior is defined by only a few data points for measurements at a distance of 20–30 cm from the gate. We note, however, that this increase in aggradation rate occurred at a time corresponding approximately to the transition between the second (constant-velocity) and third (stopping) phases of the flows. In the initially moderately expanded flows (at $E=1.09$ and 1.17) this late-stage aggradation velocity resembles that of the non-expanded flow, whereas in the most expanded flow ($E=1.35$), it does not. We stress, however, that to a first approximation the aggradation rates at each value of E are constant throughout most of the duration of sedimentation.

The deposit aggradation rates measured for the flows are now compared to those inferred from the quasi-static bed-collapse tests carried out in the flume reservoir with the lock gate closed. For an initially expanded bed collapsing at a velocity V , the deposit aggradation velocity S given by mass flux balance is $S=V/(E-1)$ (Druitt et al. 2007). Hence from equation 2 the quasi-static aggradation velocity for the ash is $S = (2.44E-2.15)/(E-1) \text{ cm s}^{-1}$. In Figure 10, deposit aggradation rates beneath the expanded flows are compared with values calculated from the settling rates measured in the collapse tests and reported earlier. Values are plotted both for the rate of initial aggradation and for a mean value for the entire duration of deposition. Irrespective of which value is used, aggradation rates beneath the $E>1$ flows agree to within measurement error with those inferred beneath quasi-static collapsing beds of the same initial expansion.

5. Discussion

Processes in the laboratory flows

The velocity fields and profiles of Figures 4–8 are to our knowledge the first measurements of internal motion in fluidized flows of hot natural ash. High-speed images show that the laboratory flows behaved to a first approximation as sheared-out collapsing beds, with a fast-moving flow below which a deposit aggraded progressively until the flow ran out of volume. The flows propagated in three distinct phases, and the measured phase-2

velocities were about $\sqrt{(2gh_0)}$, typical of inviscid dam-break flows (Roche et al., 2008). Flow at all expansions was “laminar” with no turbulent eddies significantly larger than the particle scale. It cannot be ruled out that this was in part a boundary-layer effect against the flume wall, but it is consistent with absence of surface vorticity reported by Girolami et al. (2008). An important observation is that at all expansions the frontal regions of each flow, up to 5-20 cm (0.05-0.10 s) behind the leading edge, slipped across the channel floor with only weak internal velocity gradients, whereas once deposition had begun a no-slip basal condition was established and shear was accommodated more uniformly throughout the flow. The origin of this effect is unclear and requires further study, but it may relate to differences in fluidization state between the flow head and body. In initially expanded flows, the data also revealed the existence of a superficial layer of decreasing velocity, possibly due to air drag since surface flow-velocity decrease is correlated positively with initial bed expansion. In flows of all initial expansions, the dynamics were probably constant over time at a given distance from the lock gate, as suggested by the simple upward translation of velocity profiles. When the flow traveled down the channel, the internal shear rate increased because the maximum internal velocity, about equal to the frontal velocity, was approximately constant, whereas the flow thickness decreases.

Girolami et al. (2008) estimated time-averaged deposit aggradation rates from initially expanded ash flows assuming (1) that deposition began immediately behind the flow front, and (2) that aggradation rate depended only on E and was independent of time or distance within a given flow; they then divided the final deposit thickness by total deposition time. The new data confirm these assumptions to a first approximation. In detail, however, sedimentation began 5-20 cm (0.05-0.10 s) after passage of the flow front. The dependence of aggradation rate on initial bed expansion can be explained by comparing the flow values with those of our quasi-static bed-collapse tests. As shown in Figure 10, the rates of deposit aggradation beneath the expanded ($E > 1.00$) flows determined from video analysis were similar to those inferred from the bed-collapse tests. Hence, despite rates of shear of up to 300 s^{-1} in the flows, shear had little effect on deposit aggradation rate, as also concluded by Girolami et al. (2008) based on their less accurate approach. While aggradation rate was almost independent of distance from the lock gate, there were some indications that it increased slightly with time at a given location in initially expanded flows. Note that this cannot be due to segregation of the dense SiC tracer particles towards the base of the flow, since this would result in higher initial deposition rates, the inverse of what is observed. As the aggradation rate increased approximately when the flows entered the stopping phase after about two thirds of the flow duration, this suggests a relationship between the internal dynamics of the flow and the kinematics of the front. Furthermore, the late-stage aggradation rates of the moderately expanded flows ($E = 1.09$ and 1.17) were similar to those of the non-expanded flow, which could suggest that all initially expanded flows defluidized rapidly once they had thinned beyond some threshold value. This may be consistent with the observed evolution of flow-front shape from rounded to progressively triangular, the latter being typical of non-expanded flows.

The initially non-expanded flows behaved in a similar manner to the expanded ones: shearing throughout and depositing progressively. Particle sedimentation is theoretically not possible from an initially non-expanded fluid-particle mixture. A one-dimensional granular bed just fluidized at U_{mf} defluidizes by pore-pressure diffusion, rather than settling (Druitt et al., 2007). Either defluidization of the $E = 1.00$ flow indeed took place by pore-pressure diffusion, from the base upwards, at a rate we cannot quantify, or the ash was slightly expanded by a combination of Reynolds dilation and particle agitation during shear, then underwent re-sedimentation like the other flows. If the latter is true, then an expansion of a few % is implied by extrapolation of the quasi-static curve (Figure 10), which agrees well with values reported for Reynolds dilation of sheared granular masses (Hutter et al. 2005).

One implication of this observation could be that even a flow generated from initially non-expanded (but just fluidized) ash may deposit by settling because the shear generated by flow will always slightly expand the gas-particle mixture above loose-packing. Further investigation of this possibility is required.

Implications for pyroclastic flows

The experimental results provide information on the possible flow and deposition behavior of dense pyroclastic flows propagating on a sub-horizontal slope. Fluidization in pyroclastic flows is believed to affect only the sub-mm size fractions, so that lapilli and blocks are transported in suspension or as bedload within a matrix of partially or fully fluidized ash (Sparks 1976). As our experimental ash is representative of that matrix, the behavior of the laboratory flows is likely to resemble that of natural flows containing particles of a larger size range, and this idea is supported by laboratory experiments (Roche et al. 2005). The presence of very large and/or dense clasts may, however, complicate this simple picture.

Understanding the manner in which a pyroclastic flow deposits its load is fundamental to using deposits to reconstruct eruptive processes. The deposition mechanisms of pyroclastic flows have been widely debated, possible mechanisms including frictional freezing or progressive aggradation (Sparks 1976; Branney and Kokelaar 1992, 2002, and references therein). The conceptual difference between these mechanisms is that freezing is envisaged to occur only at a late-stage following long transport, whereas progressive aggradation takes place throughout flow runout. Textural studies have been used to infer that the individual flow units and thick massive layers that constitute large ignimbrite sheets were laid down by progressive aggradation, not freezing (Branney and Kokelaar 1992, 2002). However, such flows may travel as dense turbulent suspensions, so it is less clear to what extent progressive aggradation also takes place in pyroclastic flows of small volume in which whole-body turbulence is less likely (e.g., Sparks et al. 1997). However, the experiments of Girolami et al. (2008) and this paper now show that even non-turbulent dam-break flows of ash as thin as a few cm deposit progressively. Moreover, this behavior also characterizes even the initially non-expanded ash flows, so it seems to be a general feature of dense gas-particle flows, irrespective of thickness, expansion or degree of turbulence.

The apparent insensitivity of deposit aggradation rate to shear may offer a means of parameterizing deposit aggradation rates in flow models by using sedimentation rates measured in quasi-static rigs. Mathematical models taking into account progressive deposition have been developed for granular flows, but only for dry (i.e., non-fluidized) flows and assuming empirical aggradation rates (Doyle et al. 2007). On the other hand, some numerical models simulate (partially) fluidized geophysical flows, but do not yet include progressive deposition (Iverson and Denlinger 2001; Denlinger and Iverson 2004). In this context, the results presented in this paper could serve as a guide for including deposit aggradation in models of fluidized flows. Such an approach would be limited to the modelling of relatively dense fluidized flows propagating on a sub-horizontal slope and in which turbulence is absent on a scale comparable to that of the flow thickness.

The experiments also provide insight into the way in which shear may be accommodated vertically in different parts of a pyroclastic flow. The bases of pyroclastic flow deposits are commonly erosional on the underlying substrate, especially on steep slopes, the substrates exhibiting deep erosional channels, striations, furrows and percussion marks (Rowley et al. 1982; Sparks et al. 1997; Cole et al. 2002; Pittari and Cas 2004). These features show that pyroclastic flows can exert high shear stresses on the ground over which they travel. The erosion and incorporation of substrate lithic clasts, as well as the shear-laminations

common in some ignimbrite basal layers are also indicative of high basal shear (Buesch 1992; Susuki-Kamata 1998; Branney and Kokelaar 2002). Erosional features at Lascar Volcano were interpreted to form when highly concentrated flows slid over the bedrock, and they were favored by basal segregation of lithic clasts as well as flow acceleration caused by topographic restrictions and local steep slopes (Sparks et al. 1997). Similar conclusions have been reached for the Abrigo Ignimbrite on Tenerife, where impact and sole marks are interpreted as the consequence of the passage of a highly energetic flow head enriched in pebble- to cobble-sized lithic clasts (Pittari and Cas 2004). In contrast, the typically massive interiors of flow units preserve evidence only for lower levels of shear at the aggrading depositional surface, such as magnetic fabrics, clast imbrication and flow-parallel orientation of elongated particles, crystals and logs (e.g., Suzuki and Ui 1982; Knight et al. 1986; Potter and Oberthal 1987; Hughes and Druitt 1998 and references therein). Possible features indicative of intense shear, such as shear laminations and truncated clasts are generally absent within the massive interiors of flow units. This suggests that high basal shear stresses are probably limited to the frontal regions of pyroclastic flows and that, once the deposit starts to aggrade, shear stress at the base of the moving flow (i.e., the depositional surface) falls to lower values.

Velocity profiles associated with the leading edges of the laboratory flows show that the flow front slides over the flume floor. It is therefore inferred that the flow front exerts a strong shear stress (at the scale of the flow) on its substrate. Although the effects of this basal shear are not visually evident because the floor is rigid, high basal stress is inferred from the very steep velocity gradient at the base of the flow front. In a natural pyroclastic flow such a process might give rise to strong substrate erosion, as commonly observed. Frontal sliding has been proposed previously for highly concentrated pyroclastic flows with poorly-fluidized bouldery snouts (Iverson and Vallance 2001 and references therein), but our experiments show that it can occur even in the absence of coarse segregated particles. The experiments also show that as the flow front passes by and sedimentation commences, the flow develops a no-slip boundary with its aggrading deposit and shear is accommodated more pervasively throughout the flow. Textural evidence for shear may therefore be expected to be less common in the interiors of flow deposits, as is indeed the case.

Conclusions

We carried out experiments on dam-break flows of initially fluidized volcanic ash in order to better understand the transport and sedimentation processes in dense pyroclastic flows propagating on sub-horizontal slopes. The ash was representative of the matrices of natural flows and was expanded to amounts of up to 35% before release. The internal kinematics of the flows was documented by measuring the velocity fields of the constituent particles and their spatial and temporal variations. High-speed videos were acquired at 1000 frames per second, and subsequently analyzed using a particle-tracking algorithm.

The results revealed that the experimental flows behaved to a first approximation as sheared-out collapsing beds, with a fast-moving flow overriding a basal deposit that aggraded progressively until the flow was consumed. The overriding flow was non-turbulent and pervasively sheared, with a slightly concave-upward velocity profile. In initially expanded flows, the maximum internal velocity was close to that of the flow front, with shear rates up to $\sim 300 \text{ s}^{-1}$; some decrease in velocity was observed near the flow surface, possibly due to air drag. Flows of all initial expansions were characterized by a frontal region that slid across the floor of the flume on a thin, highly sheared basal layer. Deposit aggradation commenced $\sim 0.05\text{--}0.10 \text{ s}$ ($\sim 5\text{--}20 \text{ cm}$) behind the flow front and took place at a rate of a few cm per second that was similar to that inferred for quasi-static bed collapse tests at the same values of initial expansion. Once deposition had begun, a no-slip condition was established at the base of the

flow. At a given distance from the lock gate, the velocity profile of the flow was translated upward as the deposit aggraded, suggesting time-invariant flow dynamics. The aggradation rate decreased as the initial bed expansion increased, and (within a flow of given expansion) was independent of the distance travelled. It was approximately constant with time at a given location, though it apparently increased when the flows entered their last, decelerating phase of emplacement. Initially non-expanded flows deposited progressively in a manner similar to initially expanded ones, even though particle sedimentation is theoretically not possible from the packed state. This suggests that the non-expanded flows may have undergone shear-induced dilation of a few percent during initial slumping.

Our study has some implications for our understanding of the kinematics of dense pyroclastic flows in nature. First, it shows that progressive aggradation of a basal deposit and pervasive shear of the overlying flow are likely mechanisms. Second, substratum erosion and lithic incorporation observed in the field could be the consequences of intense shear stresses at the base of a sliding flow front. Third, the deposit aggradation rates essential for the modeling of pyroclastic flows may in principle be determined from simple quasi-static bed-collapse tests.

Acknowledgments

We thank J. L. Fruquière and G. Carazzo for technical assistance throughout the experiments involving the high-speed video camera.

References

- Branney MJ, Kokelaar MJ (1992) A reappraisal of ignimbrite emplacement: progressive aggradation and changes from particulate to non-particulate flow during emplacement of high-grade ignimbrite. *Bull Volcanol* 54: 504-520
- Branney MJ, Kokelaar P (2002) Pyroclastic density currents and the sedimentation of ignimbrites. *Geol Soc Lond Memoir* 27, 152 pp.
- Buesch DC (1992) Incorporation and redistribution of locally derived lithic fragments within a pyroclastic flow. *Geol Soc Am Bull* 104: 1193-1207
- Cole PD, Calder ES, Sparks RSJ, Clarke AB, Druitt TH, Young SR, Herd RA, Harford CL, Norton GE (2002) Deposits from dome-collapse and fountain-collapse pyroclastic flows at Soufrière Hills Volcano, Montserrat. *Geol Soc Lond Memoir* 21: 231-263
- Corpetti T, Heitz D, Arroyo G, Ménin E, Santa-Cruz A (2006) Fluid experimental flow estimation based on an optical-flow scheme. *Exp Fluids* 40: 80-97
- Denlinger RP, Iverson RM (2004) Granular avalanches across irregular three-dimensional terrain: 1. Theory and computation. *J Geophys Res* 109: F01014, DOI 10.1029/2003JF000085
- Doyle E, Huppert HE, Lube G, Mader H, Sparks RSJ (2007) Static and flowing regions in granular collapses down channels: insights from a sedimenting shallow water model. *Phys Fluids* 19: 10-21
- Davies R, Kaye B (1971) Experimental investigation into the settling behaviour of suspensions. *Powder Technol* 5: 61-68
- Druitt TH (1995) Settling behaviour of concentrated, poorly sorted dispersions and some volcanological applications. *J Volcanol Geotherm Res* 65: 27-39
- Druitt TH (1998) Pyroclastic density currents. *Geol Soc Lond Spec Publ* 145: 145-182
- Druitt T., Avaré G, Bruni G, Lettieri P, Maes F (2007) Gas retention in fine-grained pyroclastic flow materials at high temperatures. *Bull. Volcanol* 69: 881-901
- Eames I, Gilbertson MA (2000) Aerated granular flow over a horizontal rigid surface. *J Fluid Mech* 424: 169-195

- Forterre Y, Pouliquen O (2008) Flows of Dense Granular Media. *Ann Rev Fluid Mech* 40: 1-24
- Freundt A, Bursik, MI, 2001. Pyroclastic flow transport mechanisms. *Developments in Volcanology* (Elsevier) 4: 173-245
- GDR MiDi (2004) On dense granular flows. *Eur Phys J E* 14: 341-365
- Geldart D (1973) Types of gas fluidization. *Powder Technol* 7: 285-292
- Gilbertson MA, Jessop DE, Hogg, AJ (2008) The effects of gas flow on granular currents. *Phil Trans Roy Soc Lond A* 366: 2191-2203
- Girolami L, Druitt TH, Roche O, Khrabrykh Z (2008) Propagation and hindered settling of laboratory ash flows. *J Geophys Res* 113 B02202 DOI:10.1029/2007JB005074
- Hoblitt RP (1986) Observations of the eruptions of July 22 and August 7 1980 at Mount St Helens, Washington. *US Geol Survey Prof Paper* 1335, 44pp
- Horn B, Schunck B (1981) Determining optical flow. *Art Int* 17: 185-203
- Hughes SR, Druitt TH (1998) Particle fabric in a small, type-2 ignimbrite flow unit (Laacher See, Germany) and implications for emplacement dynamics. *Bull. Volcanol* 60: 125-136
- Hutter K, Wang Y, Pudasaini P (2005) The Savage-Hutter avalanche model: how far can it be pushed? *Phil Trans Roy Soc Lond A* 363: 1507-1528
- Iverson RM, Denlinger RP (2001) Flow of variably fluidized granular masses across three-dimensional terrain 1. Coulomb mixture theory. *J Geophys Res* 106: 537-552
- Iverson RM, Vallance JW (2001) New views of granular mass flows. *Geology* 29: 115-118
- Knight MD, Walker GPL, Ellwood BB, Diehl JF (1986) Stratigraphy, palaeomagnetism, and magnetic fabrics of the Toba Tuffs: constraints on the sources and eruptive styles. *J Geophys Res* 91: 10355-10382
- Lettieri P, Yates J, Newton D (2000) The influence of interparticle forces on the fluidization behavior of some industrial materials at high temperature. *Powder Technol* 110: 117-127
- Levine AH, Kieffer SW (1991) Hydraulics of the August 7 1980 pyroclastic flow at Mount St Helens, Washington. *Geology* 19:1121-1124
- Lockett MJ, Al-Habbooby HM (1974) Relative particle velocities in two-species settling. *Powder Technol* 10: 67-71
- Pittari A, Cas RAF (2004) Sole marks at the base of the late Pleistocene Abrigo Ignimbrite, Tenerife: implications for transport and depositional processes at the base of pyroclastic flows. *Bull. Volcanol* 66: 356-363
- Potter DB, Oberthal CM (1987). Vent sites and flow directions of the Otowi ash flows (lower Bandelier Tuff), New Mexico. *Geol Soc Am Bull* 98: 66-76
- Rhodes MJ (1998) *Introduction to Particle Technology*. John Wiley and Sons, 315 pp.
- Roche O, Gilbertson MA, Phillips JC, Sparks RSJ (2004) Experimental study of gas-fluidized granular flows with implications for pyroclastic flows emplacement. *J Geophys Res* 109: B10201, DOI 10.1029/2003JB002916.
- Roche O, Gilbertson MA, Phillips JC, Sparks RSJ (2005) Inviscid behaviour of fines-rich pyroclastic flows inferred from experiments on gas-particle mixtures. *Earth Planet Sci Lett* 240: 401- 414
- Roche O, Montserrat S, Niño Y, Tamburrino A (2008) Experimental observations of water-like behavior of initially fluidized, unsteady dense granular flows and their relevance for the propagation of pyroclastic flows. *J Geophys Res* 113: B12203, DOI 10.1029/2008JB005664.
- Rowley PD, Kuntz MA, Macleod NS (1982) Pyroclastic-flow deposits. *US Geol Surv Prof Paper* 1250: 489-512
- Sparks RSJ (1976) Grain size variations in ignimbrites and implications for the transport of pyroclastic flows. *Sedimentology* 23: 147-188
- Sparks RSJ, Gardeweg MC, Calder ES, Matthews SJ (1997) Erosion by pyroclastic flows on Lascar Volcano, Chile. *Bull Volcanol* 58: 557-565

- Suzuki K, Ui T (1982). Grain orientation and depositional ramps as flow direction indicators of a large-scale pyroclastic flow deposit in Japan. *Geology* 10: 429-432
- Suzuki-Kamata K (1988) The ground layer of Ata pyroclastic flow deposit, southwestern Japan - evidence for the capture of lithic fragments. *Bull Volcanol* 50: 119-129
- Takahashi T, Tsujimoto H. (2000) A mechanical model for Merapi-type pyroclastic flow. *J Volcanol Geotherm Res* 98: 91-115
- Wilson CJN (1986) Pyroclastic flows and ignimbrites. *Sci Prog Oxford* 70: 171-207
- Wilson CJN (1980) The role of fluidization in the emplacement of pyroclastic flows: an experimental approach. *J Volcanol Geotherm Res* 8: 231-249

Figure captions

Figure 1. Sketch of the experimental apparatus used in this study. The widths of both the reservoir and the channel are 15 cm. Heights h_{mf} and h_0 are those of the bed at the minimum fluidization velocity (U_{mf}) and of the expanded bed (at $U_g > U_{mf}$), respectively.

Figure 2. Thickness of the basal deposit as a function of time in an initially moderately expanded flow ($E=1.17$) 20 cm from the lock gate. Comparison of data determined on the one hand by visual analysis, and on the other by using the optical-flow algorithm. The good agreement serves to validate the algorithm results.

Figure 3. Quasi-static hindered settling velocities of the SiC-laden ash as a function of initial expansion. Measurements were carried out in the flume reservoir with the lock gate closed. The data are approximated by a linear best fit $V=2.44E-2.15 \text{ cm s}^{-1}$ (black line). The grey zone shows the equivalent data on the raw ash (lacking SiC particles) used by *Girolami et al.* (2008). The effect of the SiC particles is to increase hindered settling velocity at a given expansion.

Figure 4 Velocity fields at 20-30 cm from the reservoir gate and at different times after release of the initially non-expanded flow ($E=1.00$). The dashed white line represents the interface between the flow and aggrading deposit. White lines show where the flow velocity was extracted to build the profiles of Figure 8.

Figure 5. Velocity fields at 20-30 cm from the reservoir gate and at different times after release of an initially expanded flow with $E=1.09$. The dashed white line represents the interface between the flow and aggrading deposit. White lines show where the flow velocity was extracted to build the profiles of Figure 8.

Figure 6. Velocity fields at 20-30 cm from the reservoir gate and at different times after release of an initially expanded flow with $E=1.17$. The dashed white line represents the interface between the flow and aggrading deposit. White lines show where the flow velocity was extracted to build the profiles of Figure 8.

Figure 7. Velocity fields at 20-30 cm from the reservoir gate and at different times after release of an initially expanded flow with $E=1.35$. The dashed white line represents the interface between the flow and aggrading deposit. White lines show where the flow velocity was extracted to build the profiles of Figure 8.

Figure 8. Velocity profiles determined from the velocity fields in Figures 4-7 for different initial expansions (E). (a, b) At a distance of 25 cm from the lock gate and at different times after release, and (c) at a time of 0.6 s and different distances. Heights and velocities in the flows were measured perpendicular and parallel to the depositional surface, respectively.

Figure 9. Deposit thickness as a function of time for different initial bed expansions (E) and distances from the gate. Δt is the time delay between the passage of the flow front and the onset of deposition.

Figure 10. Deposit aggradation velocity in the flows as a function of E . Black squares are the initial aggradation velocity; white triangles are the mean aggradation velocity including the slightly faster late-stage phase (cf. Figure 7). White circles are aggradation velocity inferred by mass-flux balance calculation from the quasi-static bed-collapse values of Figure 3. The curve is the best-fit function $S=(2.44E-2.15)/(E-1)$ cm s⁻¹ to the quasi-static data (see text for details). The horizontal arrow shows that deposit aggradation beneath the initially non-expanded ($E=1.00$) flow took place at a rate expected for an expansion of a few percent.

Figures

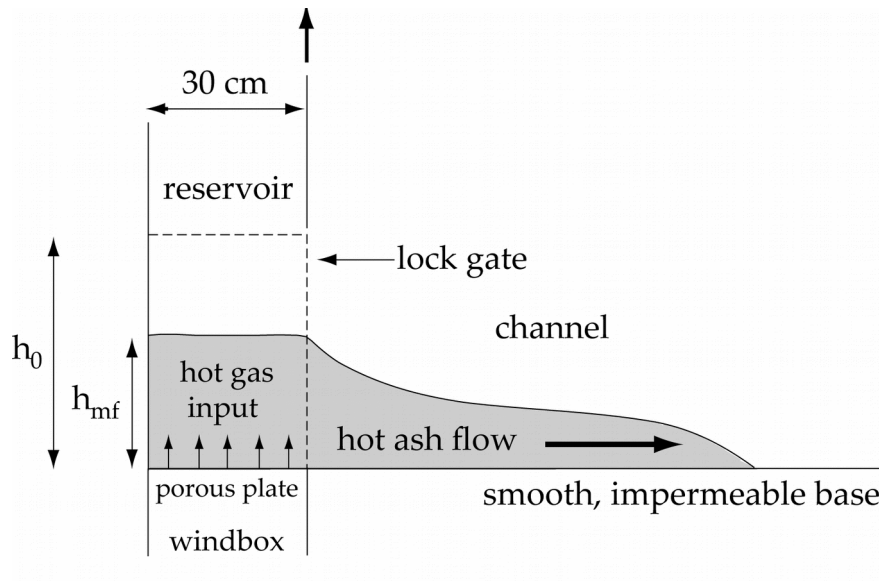


Figure 1

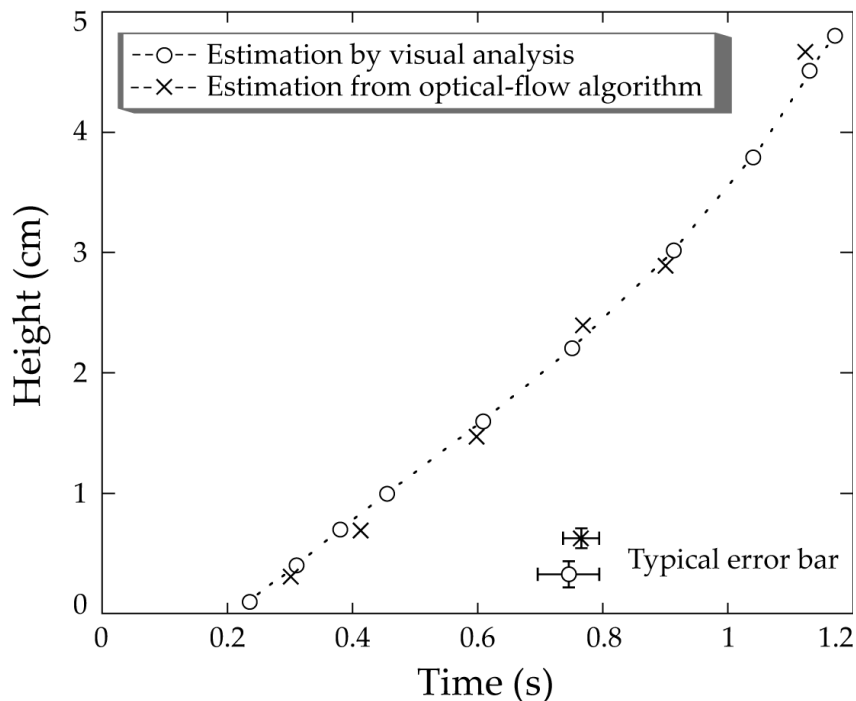


Figure 2

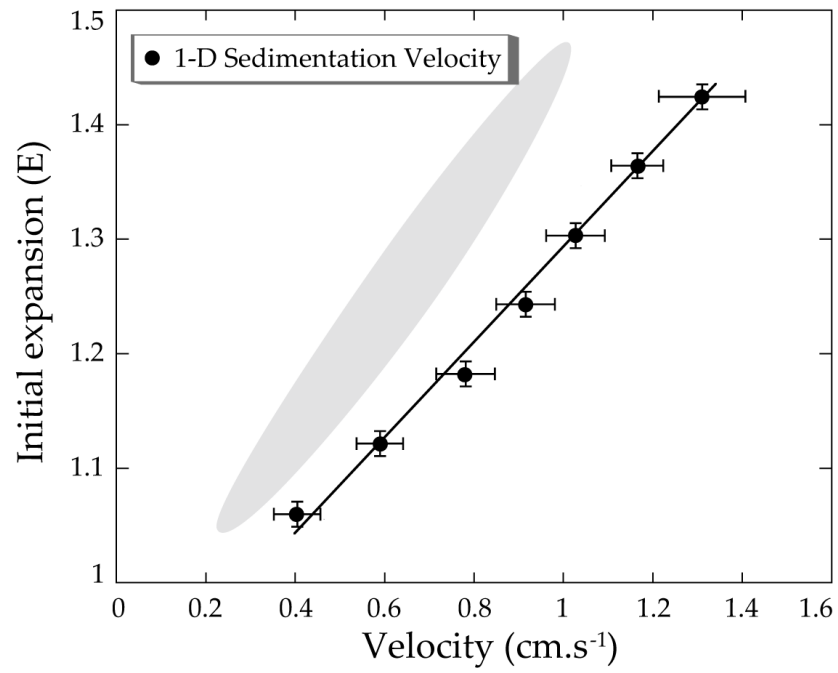


Figure 3

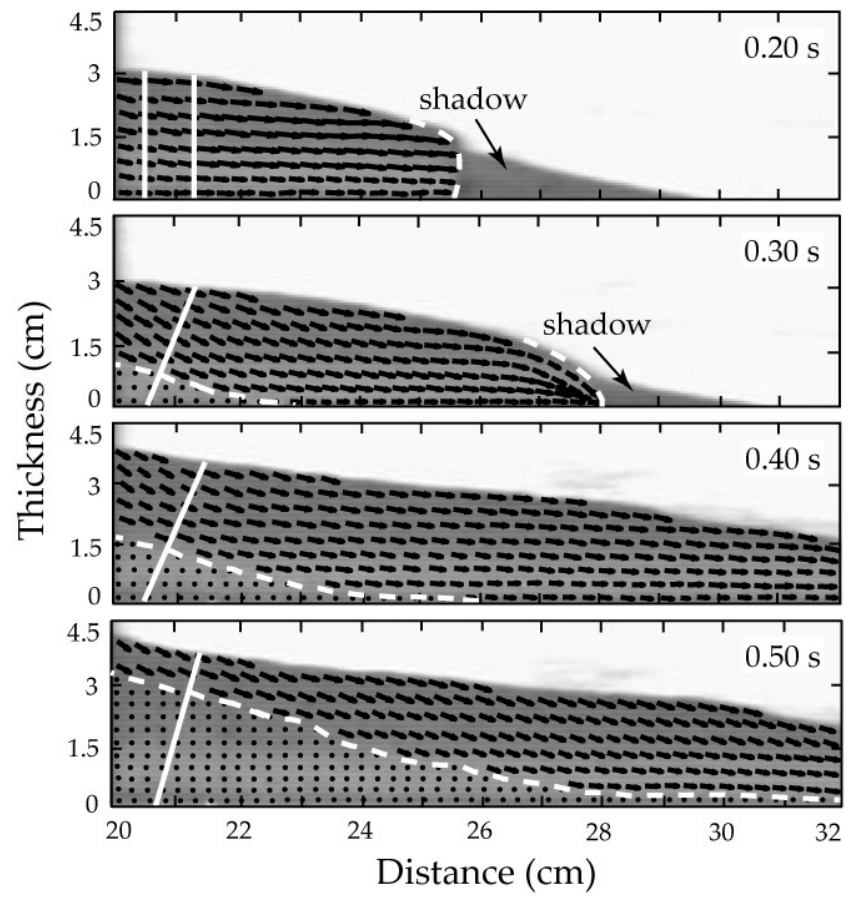


Figure 4

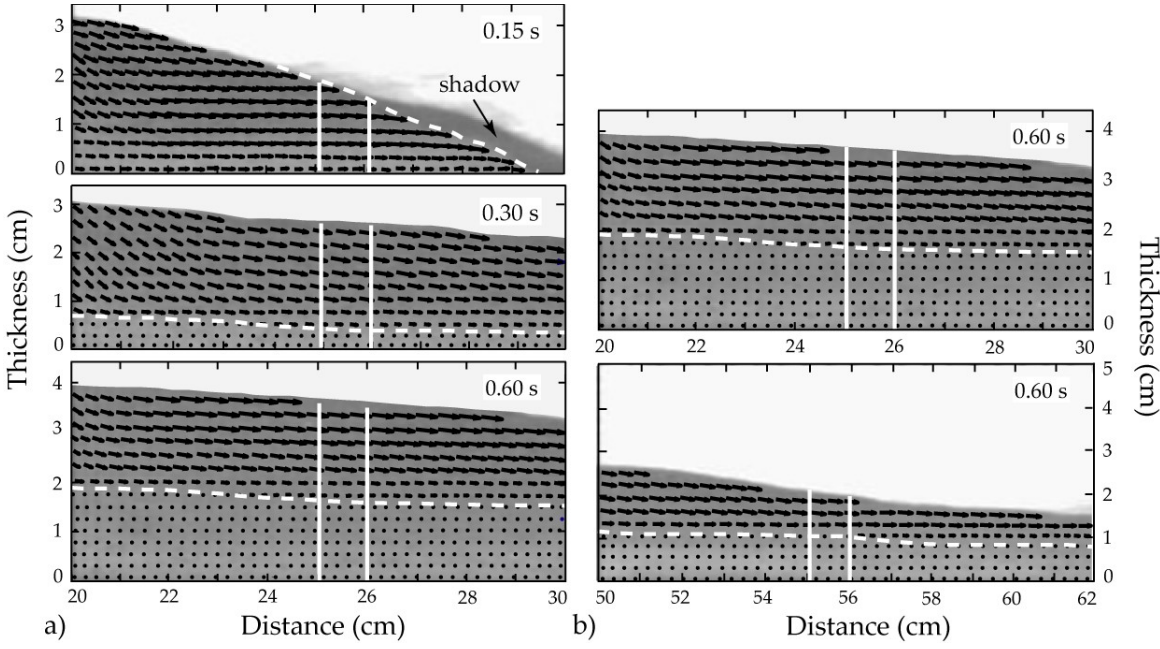


Figure 5

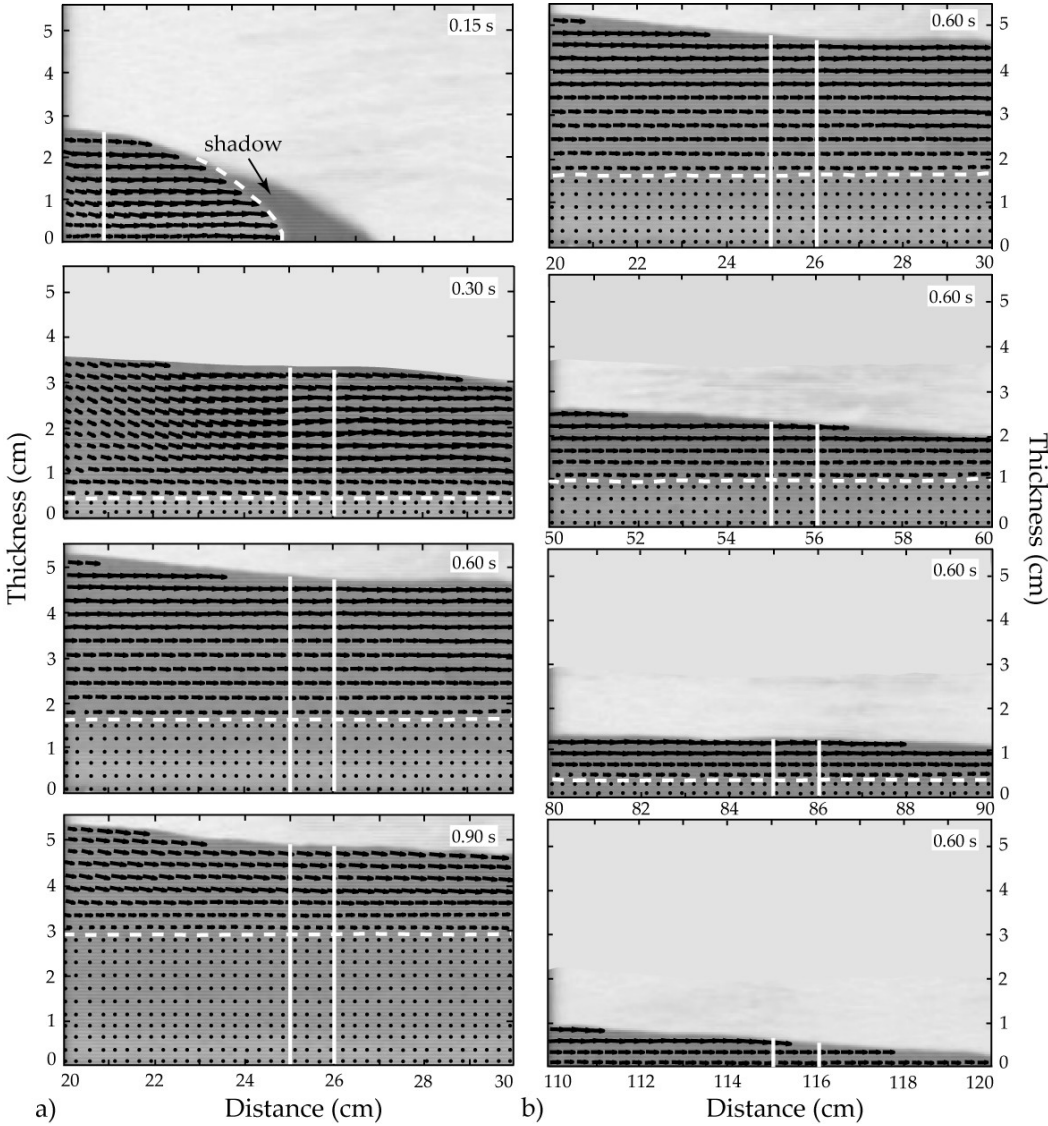
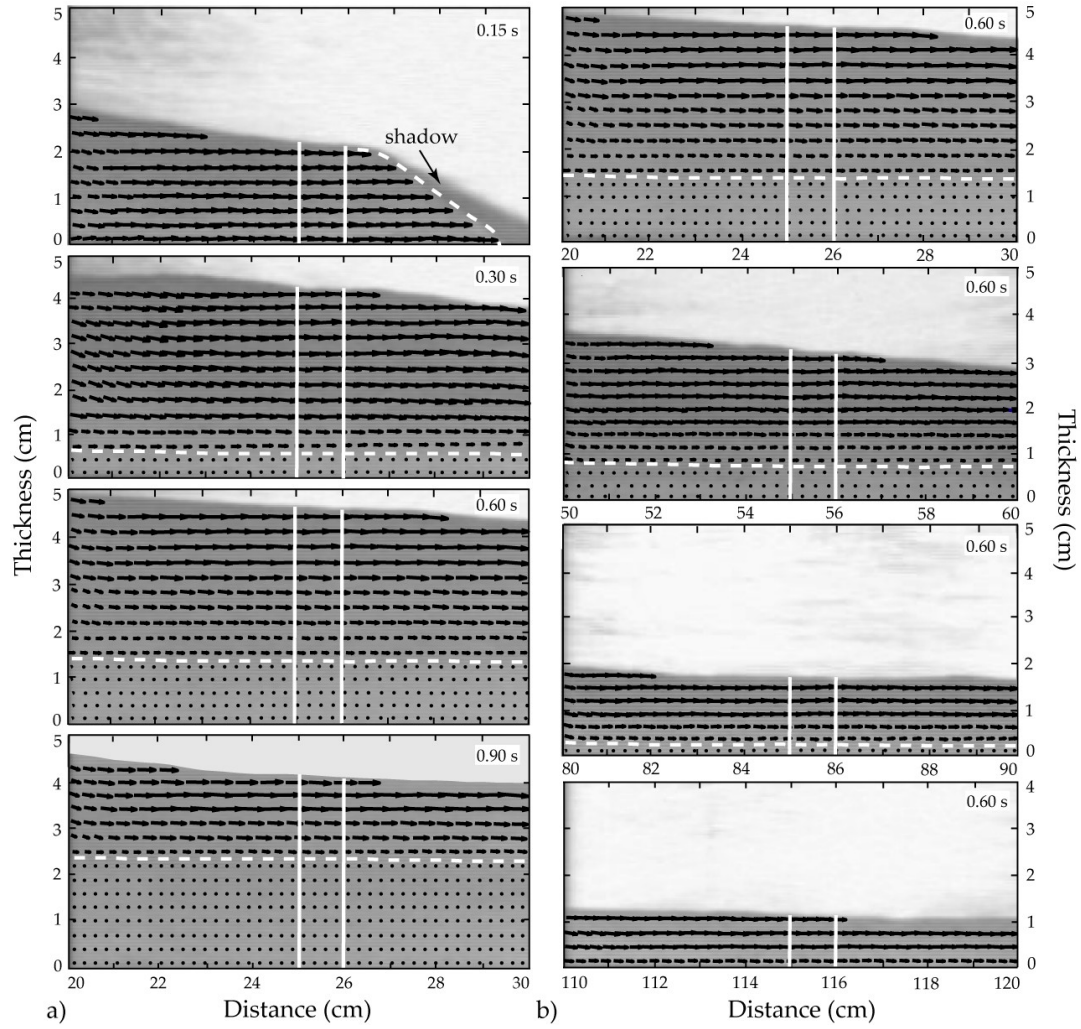


Figure 6



Figures 7

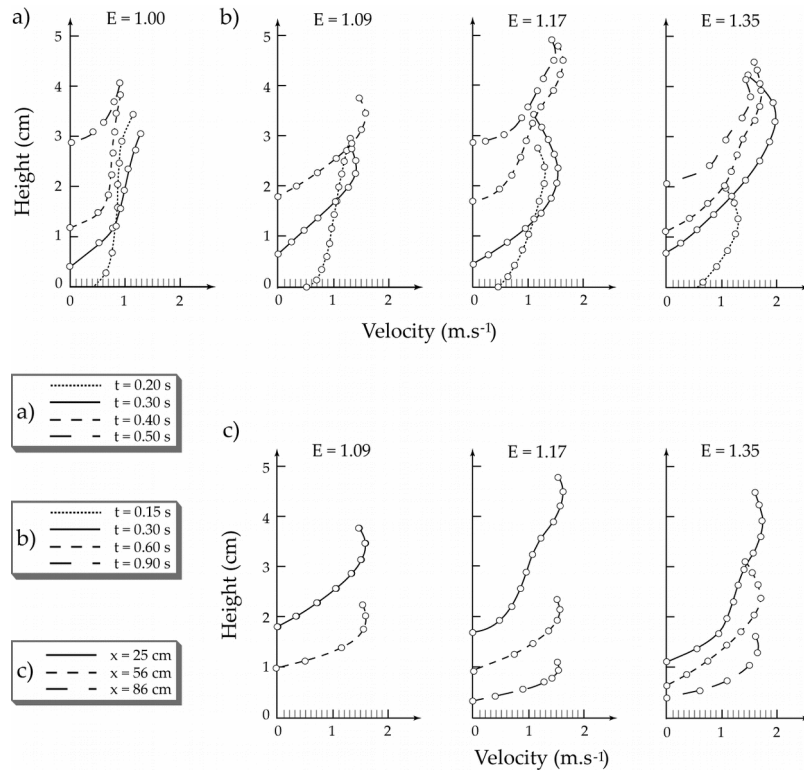
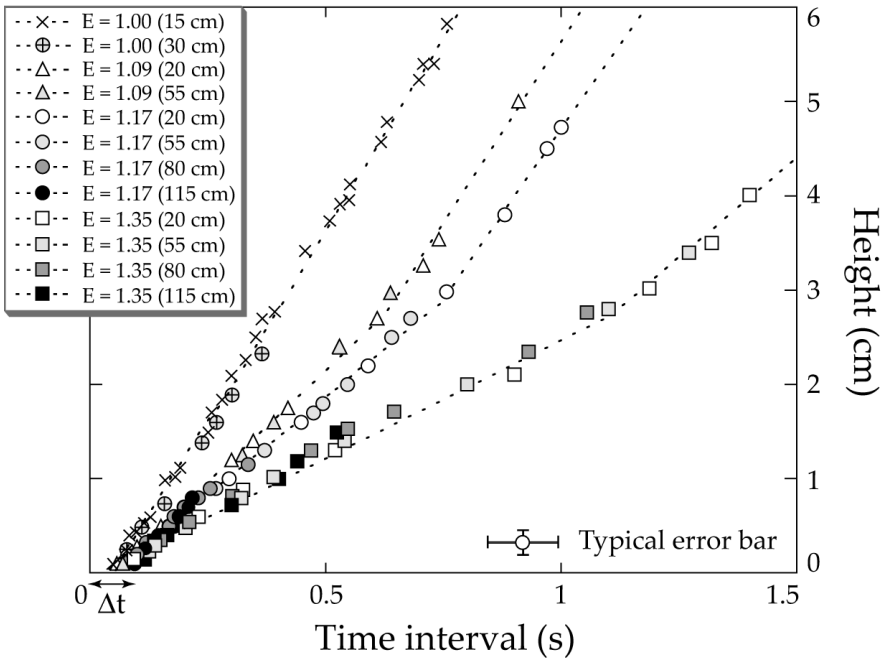
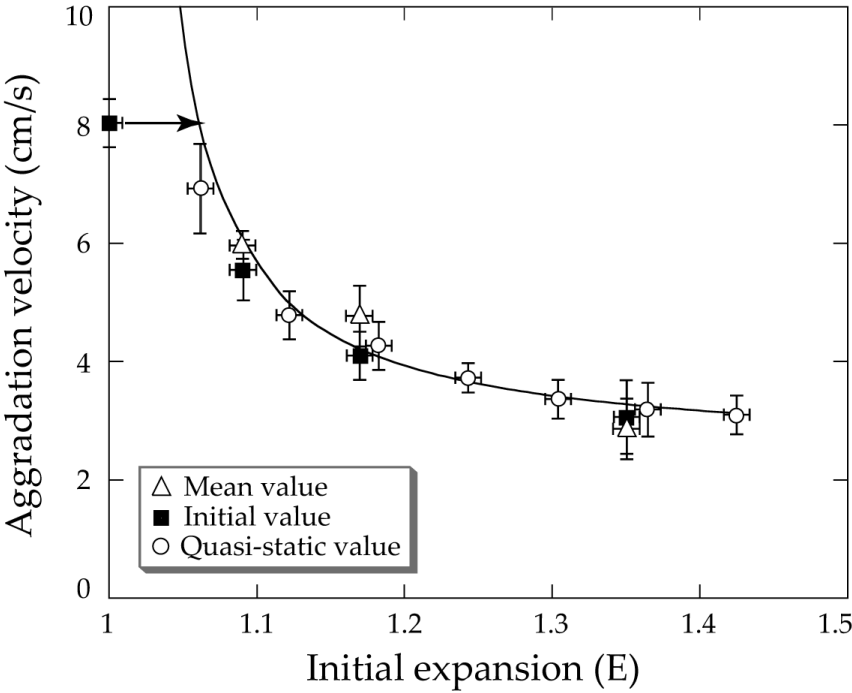


Figure 8



Figures 9



Figures 10